Polymerization of Olefins through Heterogeneous Catalysis. II. Kinetics of Gas Phase Propylene Polymerization with Ziegler–Natta Catalysts

K. Y. CHOI and W. H. RAY, *Department of Chemical Engineering, University of Wisconsin, Madison, Wisconsin 53706*

Synopsis

Propylene was polymerized in gas phase over a $TiCl_3 \cdot \frac{1}{3} AlCl_3$ (Stauffer Type AA) Catalyst with $AlEt_2Cl$ cocatalyst both with and without H_2 present. The effects of polymerization temperature, monomer concentration, catalyst composition, and hydrogen were investigated. The experiments were carried out at operating conditions approaching industrial practice.

INTRODUCTION

The gas phase polymerization of propylene is a rapidly growing and very important industrial process which may be carried out in a stirred or fluidized bed reactor. Although there is a significant patent literature (cf. Refs. 1–3 for a survey) on catalysts and processes for propylene polymerization, very little fundamental information has been published on the differences and similarities between liquid slurry and gas phase processes.[4–13]

Since the main difference between the two processes is the phase of monomer, one may assume that the catalyst will behave in a similar fashion. In many cases, the overall kinetics are indeed quite similar. However, there is also some evidence that certain aspects of polymerization kinetics of the gas phase process may differ from that of the liquid slurry process. In addition, polypropylene from the gas phase process is reported to have some properties which are distinct from those found in the slurry process product.[14]

This paper describes experimental studies of gas phase propylene polymerization kinetics over a heterogeneous Ziegler–Natta catalyst. The catalyst system used is a commercially available Stauffer AA Type 1.1 $TiCl_3 \cdot \frac{1}{3}AlCl_3$ cocatalyzed by $Al(C_2H_5)_2Cl$ (DEAC). In contrast to earlier gas phase polymerization studies reported in the literature, the present work is carried out at pressures and temperatures approaching industrial practice.

EXPERIMENTAL

Gas phase polymerization was carried out in a 1-l autoclave reactor with the experimental system shown in Figure 1. The polymerization reactor is provided with a specially designed U-shaped stirrer for uniform mixing of solids. After heating to reaction temperatures, both components of the cat-

Journal of Applied Polymer Science, Vol. 30, 1065–1081 (1985)
 CCC 0021-8995/85/031065-17$04.00

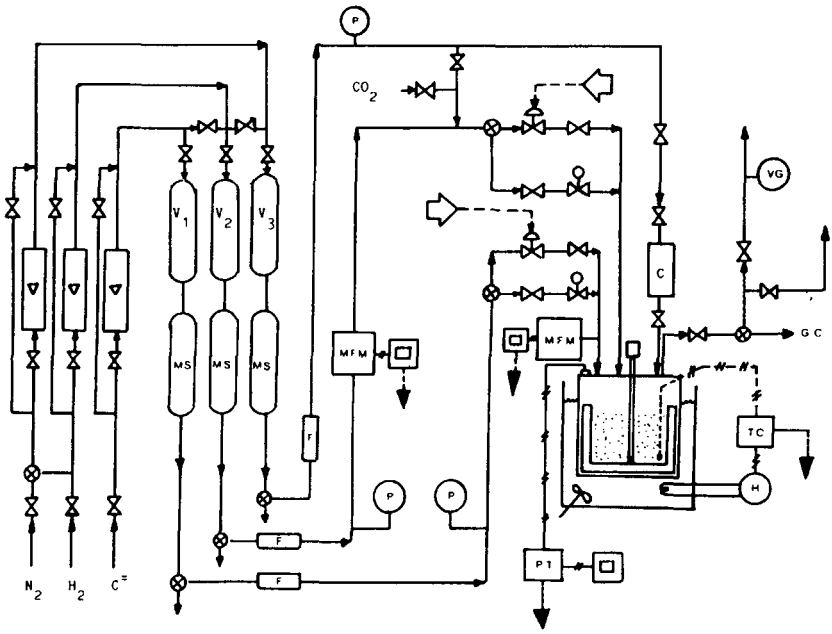

Fig. 1. Gas phase stirred bed reactor for propylene polymerization: (C) catalyst injection bomb; (F) in-line filter; (H) heater; (MFM) mass flow meter; (MS) molecular sieves; (V1, V2, V3) oxygen scavenging columns; (VG) vacuum gauge; (TC) temperature controller; (PT) pressure transducer.

alyst ($TiCl_3 \cdot \frac{1}{3}AlCl_3$ and DEAC) were mixed in a small amount of *n*-heptane and injected into the reactor. The reactor was then evacuated for approximately 1 h before monomer feed was started. The polymerization rate at each instant of time was determined by the gaseous propylene feed rate required to maintain constant pressure in the reactor. The polymer yield estimated from the polymerization rate curve agreed to within $\pm 5\%$ with the actual gravimetrically determined yield. To promote a uniform distribution of catalyst, a small volume of $\sim$1 mm glass beads was added to the reactor before injecting the catalyst mixture. When hydrogen was used, the reactor was first charged with hydrogen to the desired hydrogen partial pressure, and then the total pressure was raised to the desired reaction pressure by adding propylene. The polymer recovered from the reactor was washed with methanol, filtered, dried, and weighed to determine polymer yield. The tacticity of the polymer was measured by extracting the purified product with boiling *n*-heptane for 6 h in a Soxhlet extractor. The results are reported as percentage heptane insolubles. The molecular weight and MWD of the polymer were determined by gel permeation chromatography. More details of experimental procedure may be found in Ref. 15.

RESULTS AND DISCUSSION

Effect of Polymerization Temperature.

Experimental runs were carried out at four different temperatures (32°C, 50°C, 70°C, and 90°C) to determine the effect of reaction temperature

on the polymerization rate and polymer properties. Figure 2 shows the observed reaction rate curves. The rates (g poly/g cat · h) are completely compatible with liquid phase polymerization rates when one considers the reduced monomer concentration in the gas phase. Note that the reaction rate rapidly reaches a maximum and then gradually declines. The results from our experiments are in contrast with those of Keii and co-workers,[4-7] who observed gradually increasing rate curves ("acceleration type") when polymerizing propylene over $TiCl_3 \cdot \frac{1}{3}AlCl_3$ with DEAC as a cocatalyst. It seems likely that their acceleration type kinetic curves are due to the mild reaction conditions (i.e., low pressure and low temperature) used in their experiments.

The yields from these runs performed at different temperatures may be used to estimate an overall activation energy for gas phase polymerization. Assuming a first order reaction rate expression, one obtains the following[16]:

$$\ln \frac{\overline{R}_p}{[M]_b} = -\frac{E_{ov}}{RT} + \ln\left(\frac{1}{t_f}\int_0^{t_f} k_{ov}[C^*]_0\, dt\right) \tag{1}$$

where $\overline{R}_p$ is an average polymerization rate, $[M]_b$ a bulk monomer concentration, E_{ov} an overall activation energy, t_f a reaction time, k_{ov} a preexponential factor of rate constant, and $[C^*]_0$ the maximum number of active sites available. Here, the bulk phase propylene concentration $[M]_b$ is estimated by the Peng–Robinson equation of state[17]:

$$P = \frac{RT}{v - b} - \frac{a(T)}{v(v + b) + b(v + b)} \tag{2}$$

Our polymerization rate data were used to construct the Arrhenius plot shown in Figure 3. Because of catalyst deactivation the polymerization rate declines rapidly during the early stages of polymerization; thus the average rate ($\overline{R}_p$) is somewhat dependent on the duration of experiment. Note that,

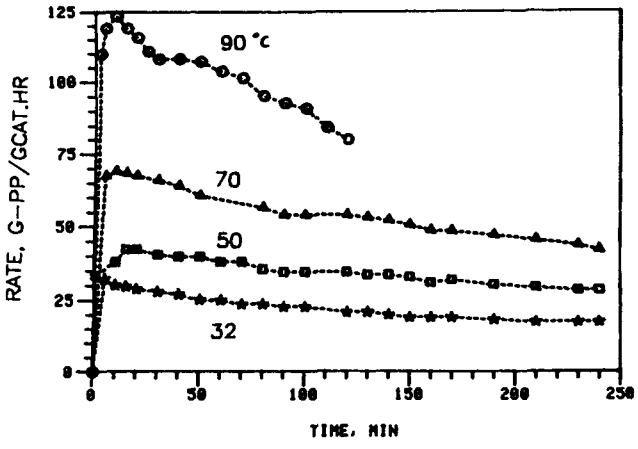

Fig. 2. Effect of polymerization temperature on the reaction rate, [Al]/[Ti] = 3.68, P = 7.5 atm.

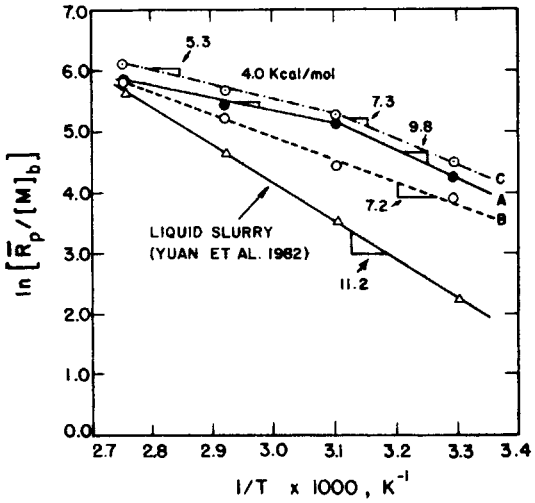

Fig. 3. Arrhenius plot for low pressure slurry reactor and gas phase polymerization; slurry: average rate over 4 h; gas phase: $P = 7.5$ atm, [Al]/[Ti] = 3.68, (A) average rate over 1 h, (B) average rate over 4 h, (C) initial rate.

considering average rates over 4 h, slurry polymerization results with the same catalyst system yield an overall activation energy of 11.2 kcal/mol,[16] while the gas phase polymerization results for a 4 h run show an activation energy of 7.2 kcal/mol. Of some interest is the apparent break in the curve when 1 h average rates are used. This shows an activation energy of 9.8 kcal/mol at low temperatures and activation energy of 4.0 kcal/mol above 50°C. A similar change in slope is also found when the initial reaction rates, obtained by extrapolating the rate curves to zero time, are used. Although slight changes in slopes are noticeable, it appears that the activation energy for gas phase propylene polymerization is always smaller than that for liquid slurry polymerization.

The activation energy values obtained from the present study are in general agreement with those obtained by several other workers as indicated in Table I. The retardation of the polymerization rates at high temperatures may be attributed to two factors: (i) increased intraparticle mass

TABLE I
Reported Activation Energies (E_a) in Propylene Polymerization

Workers	Catalyst system	E_a (kcal/mol)	
		Slurry	Gas
Natta[18]	α-$TiCl_3$/TEA	10	
Keii et al.[4,7,19]	$TiCl_3$/DEAC	13.5	12.0
	$TiCl_3$/TEA		
Grigorev et al.[13]	$TiCl_3$/TEA	11.5–12.5	4.9–5.7
Wisseroth[20,21]	Ziegler catalyst		3–5
Brockmeier[22]	$TiCl_3$/TEA		14.5
Yuan et al.[16]	δ-$TiCl_3$ · $\frac{1}{3}AlCl_3$/DEAC	11.2	
Doi et al.[23]	$MgCl_2$ supported		
	$TiCl_4$/TEA/EtBz		5.3
This work	δ-$TiCl_3$ · $\frac{1}{3}AlCl_3$/DEAC		4–10

transfer resistance and (ii) rapid deactivation of polymerization centers at high temperatures. It is well known that where intraparticle diffusion limits the overall reaction rate, the apparent activation energy in the high temperature region is reduced from the intrinsic activation energy.

Grigorev et al.[13] attributed the low activation energy of gas phase polymerization to the absence of monomer–solvent interactions. They postulate that if the rate determining step is the adsorption and coordination of monomer molecules at the catalyst surface, the solvent molecules present in liquid slurry reaction may cause steric hindrance, resulting in an increase in the energy barrier.

Figure 4 shows the polymer tacticity (% heptane insolubles) as a function of reaction temperature for three cases: (i) gas phase reactor with DEAC (present work), (ii) gas phase reactor with TEA,[4] and (iii) slurry phase reactor with DEAC.[16] The tacticity for the gas phase reactor is % heptane insolubles for total polymer product while for the slurry phase reactor, the tacticity is for the solid particle product and does not include the low molecular weight and atactic material dissolved in the reactor diluent. It is interesting that the gas phase polymer produced with DEAC has a tacticity of 95% based on total polymer—comparable to the solid particle fraction in slurry and much higher than total polymer tacticity in slurry (which is normally 80–90% below 70°C). As expected, the tacticity of the gas phase product with TEA[4] is lower than with DEAC. Note that the effect of temperature on the tacticity is severe above 70°C for slurry polymerization[16] and only slight for gas phase polymerization with DEAC up to 90°C. This is in qualitative agreement with earlier results of Keii and Doi[4] using TEA.

Effect of Monomer Concentration

The effect of monomer concentration (partial pressure) was investigated by conducting polymerizations at four different pressures (7.5, 6.2, 4.8, and 3.1 atm). Figure 5 shows the polymerization rate curves observed. Note that

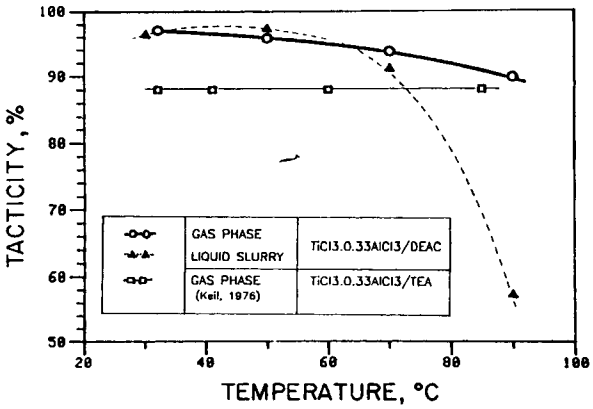

Fig. 4. Effect of temperature on polymer tacticity (% heptane insolubles) for (○) gas phase reactor with DEAC ([Al]/[Ti] = 3.68, P = 7.5 atm), (□) gas phase reactor with TEA,[4] (▲) slurry phase reactor[16] with DEAC. For the gas phase reactor, tacticity is in terms of % heptane insolubles for total polymer product. For liquid phase reactor, the tacticity is % heptane insolubles of the solid particle product.

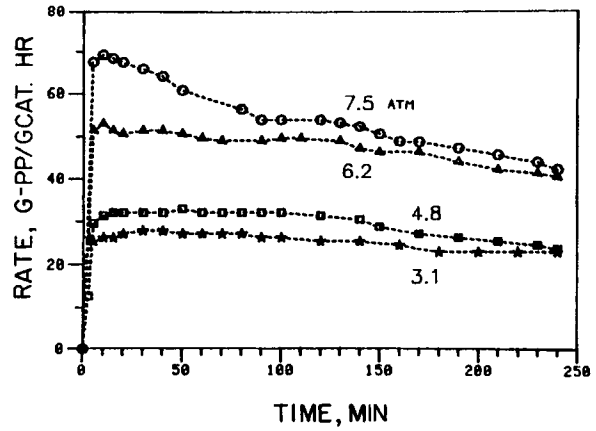

Fig. 5. Effect of reactor pressure on polymerization rate at 70°C, [Al]/[Ti] = 3.68.

the initial rate peak becomes more pronounced at high monomer pressure (i.e., high reaction rate). Figure 6 demonstrates the first order dependence of the overall polymerization rate on monomer concentration. As indicated in Figure 7, reaction pressure has a small effect on polymer tacticity.

Effect of Aluminumalkyl Cocatalyst

The composition of catalyst represented by an [Al]/[Ti] molar ratio is an important reaction parameter in the polymerization of propylene. Figure 8 shows the observed reaction rate curves for five different [Al]/[Ti] ratios with $TiCl_3 \cdot \frac{1}{3}AlCl_3$ concentration held constant. Figure 9 shows that the effect of [Al]/[Ti] ratio on catalyst yield in gas phase polymerization reaches diminishing returns at about [Al]/[Ti] $\approx$ 5. Note that increasing the [Al]/[Ti] ratio results in a more rapid initial rate, even though the yield increase may be marginal.

Polymer tacticity increases to an asymptotic value with increasing [Al]/[Ti] ratios as indicated in Figure 10. The low tacticity at low [Al]/[Ti] ratios

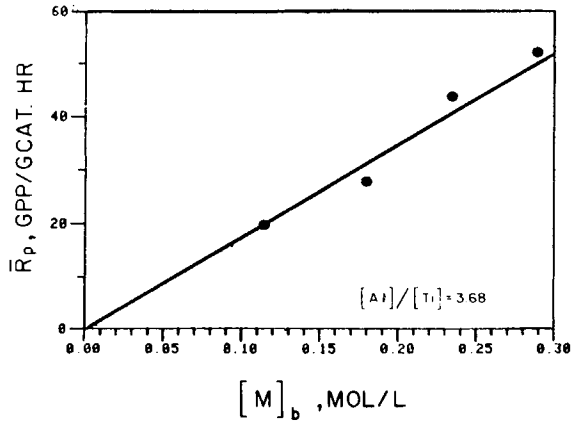

Fig. 6. Illustration of first order dependence on gas phase monomer concentration (70°C), [Al]/[Ti] = 3.68.

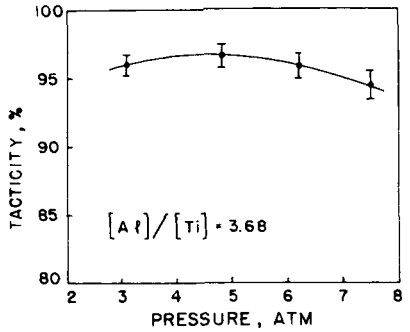

Fig. 7. Effect of pressure on polymer tacticity (% heptane insolubles) at 70°C $P = 7.5$ atm, [Al]/[Ti] = 3.68.

(e.g., [Al]/[Ti] = 1.84) suggests that atactic sites may be preferentially formed when the aluminumalkyl concentration is not sufficiently high to saturate all possible catalytic sites.

If the active site is formed by the adsorption of aluminumalkyl compound on the surface of $TiCl_3$ catalyst, the following Langmuir adsorption isotherm is valid:

$$[C^*]_0 = [N^*] \frac{K_A[Al]}{1 + K_A[Al]} \tag{3}$$

where $[C^*]_0$ is a concentration of active Ti-sites, $[N^*]$ a concentration of total Ti-sites, and K_A is an adsorption equilibrium constant. If the rate decay is assumed to follow a first-order deactivation mechanism, the catalyst site concentration at time t takes the following form:

$$[C^*] = [N^*] \frac{K_A[Al]}{1 + K_A[Al]} e^{-\lambda_d' t} \tag{4}$$

where λ_d' is a deactivation constant. Then, the rate expression becomes

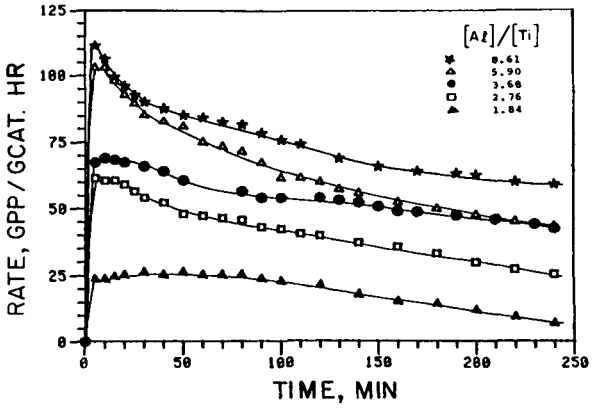

Fig. 8. Polymerization rate history at varying aluminumalkyl concentration; $TiCl_3$ = 0.3 g, T = 70°C, P = 7.5 atm. [Al]/[Ti]: (✱) 8.61; (△) 5.90; (●) 3.60; (□) 2.76; (▲) 1.84.

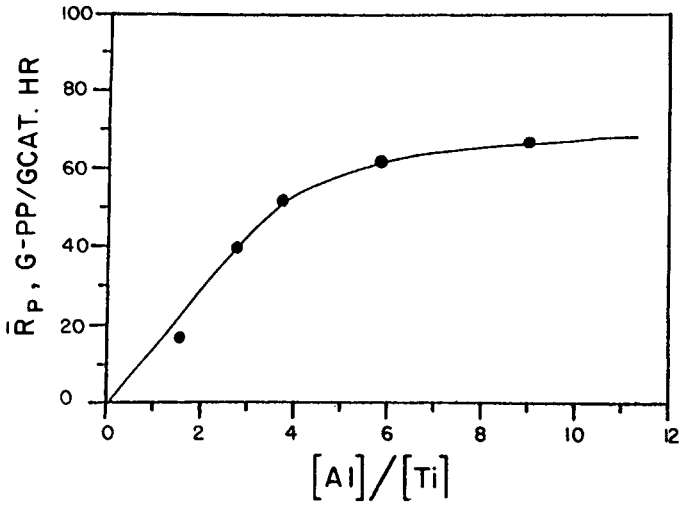

Fig. 9. Effect of aluminumalkyl concentration on average rate of polymerization, 70°C, 7.5 atm, [Ti] = 1.5 mmol. δ-$TiCl_3$ · 1/3 $AlCl_3$-DEAC.

$$R_p = k_{ov}(T)[N^*]\left(\frac{K_A[Al]}{1 + K_A[Al]}e^{-\lambda_d t}\right)[M]_b \tag{5}$$

When the concentration of titanium ([Ti]) is held constant, eq. (5) can be rearranged into the following form:

$$R_p = k_{ov}[N^*]\left[\frac{K'_A\{[Al]/[Ti]\}}{1 + K'_A\{[Al]/[Ti]\}}e^{-\lambda_d t}\right][M]_b \tag{6}$$

To compare initial rate data with the model, eq. (6) may be rearranged as follows:

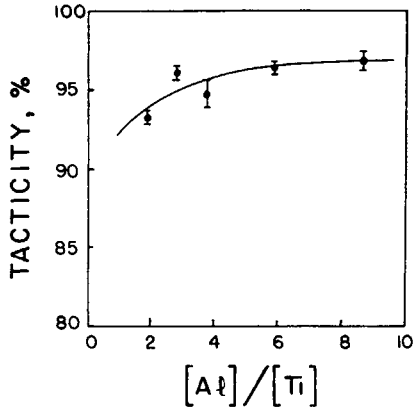

Fig. 10. Effect of [Al]/[Ti] ratios on polymer tacticity (% heptane insolubles) at 70°C, 7.5 atm.

$$\frac{1}{R_p(0)} = \frac{1}{k_{ov}[N^*][M]_b}\left[1 + \left(\frac{1}{K'_A}\right)\frac{1}{\beta}\right] \tag{7}$$

where $R_p(0)$ represents the initial polymerization rate and β = [Al]/[Ti].

Figure 11 is a plot of $1/R_p(0)$ vs. $1/\beta$ constructed from the experimental data shown in Figure 8. Note that with the exception of one data point (A: [Al]/[Ti] = 1.84) the adsorption model data is fit quite well. Data point A at the lowest ratio of (Al/Ti) is probably in error because when a low level of alkyl is used, a much larger fraction is used for scavenging trace quantities of O_2 and H_2O and less is available for site activation. The postulated model seems valid over the range [Al]/[Ti] = 2.5–10.0 with an adsorption equilibrium constant (K'_A) of 0.141 (mol Ti/mol Al).

Effect of Hydrogen

Hydrogen is known as a very efficient chain transfer agent for olefin polymerization. Experiments were performed at different hydrogen partial pressures to investigate the effect of hydrogen on the polymerization rate. Figure 12 shows the average reaction rate as a function of hydrogen partial pressure with the propylene partial pressure constant at 6.7 atm. When the hydrogen concentration is low, the overall polymerization rate increases slightly; however, a further increase in the hydrogen concentration results in a decrease in the reaction rate. Yuan et al.[16] also observed that the reaction rate increased slightly with H_2 addition in heptane slurry polymerization with the same catalyst system when the concentration of dissolved H_2 was low (i.e., $X_{H_2} = 0.002$).

Figure 13 demonstrates the rate-suppressing effect of H_2 when its concentration is relatively high. Here, hydrogen was added to the reactor during the course of polymerization with propylene partial pressure held

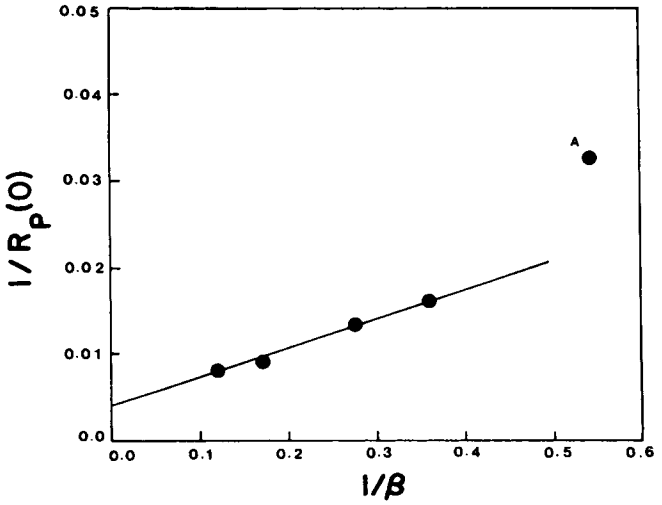

Fig. 11. Test of kinetic model [eq. (7)]; Stauffer AA Type 1.1/DEAC, 70°C, 7.5 atm.

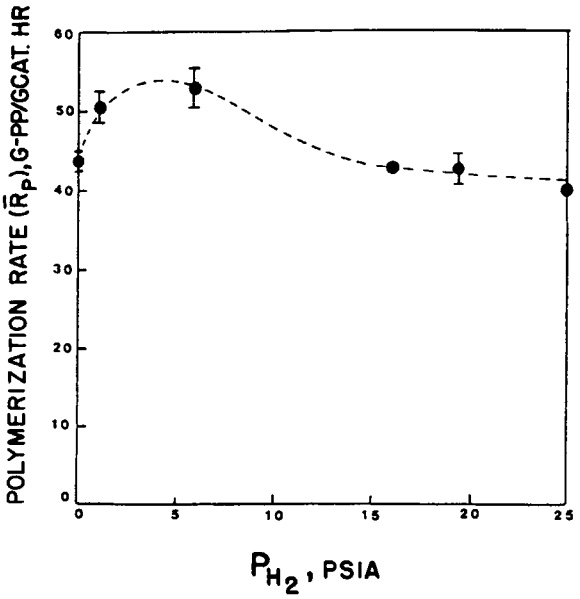

Fig. 12. Effect of hydrogen on the polymerization rate, 70°C, $P_{C_3H_6}$ = 98 psia, [Al]/[Ti] = 5.0. Stauffer AA Type 1.1 DEAC.

constant. Note that when hydrogen is removed from the reactor and the reaction is resumed by adding pure propylene, the original polymerization rate is quickly established. This indicates that the effect of hydrogen on reaction rate is reversible. The rate decrease at high H_2 concentration was also observed by other workers for liquid slurry polymerization.[9,18,25] Although the cause of this phenomenon is not yet well understood, some authors have attributed the rate decrease to slow addition of olefin monomer to the catalyst—H bond (which results from chain transfer), or to a side reaction such as partial hydrogenation of aluminumalkyl.[18]

There are also a number of other observations reported in the literature. For liquid slurry polymerization of propylene, several workers found in-

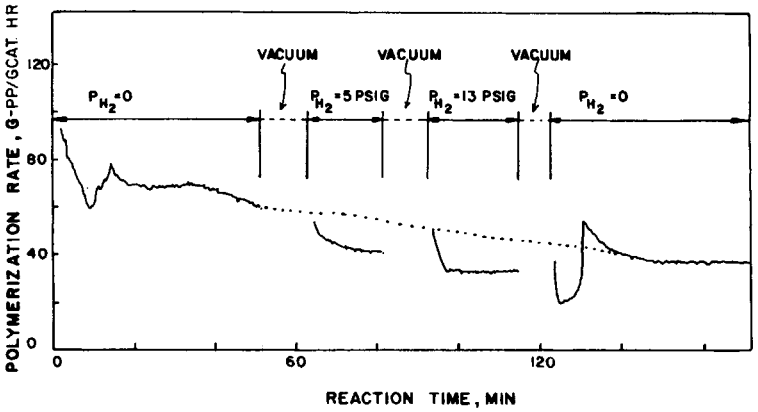

Fig. 13. Effect of hydrogen on the polymerization rate (70°C), $P_{C_3H_6}$ = 98 psig, [Al]/[Ti] = 5.0.

creased activity with H_2 addition, depending on the type of diluent and the form of reduced $TiCl_3$ catalyst.[10,26,27] For example, Okura et al.[10] observed that addition of H_2 enhanced the reaction rate when toluene instead of heptane was used as a diluent, with Stauffer AA type catalyst. They suggest that new active centers are formed on the surface of $TiCl_3$ as a result of washing out of $AlCl_3$ by toluene followed by reduction of the fresh surface by $Al(C_2H_5)_2Cl$ and hydrogen.

Recently, Guastalla and Giannini[28] investigated the influence of H_2 on the polymerization of propylene and ethylene with a $TiCl_4/MgCl_2/AlEt_3$ catalyst. They observed enhancement of reaction rate at low H_2 concentrations. However, at low temperature (17°C) H_2 did not boost the catalyst activity while still strongly decreasing the molecular weight of the polymer. From this observation, they concluded that the chain regulating ability of H_2 is not related to its activating effect.

Pijpers and Roest[27] explain the rate increase on hydrogen addition in 4-methyl-1-pentene polymerization over γ-$TiCl_3 \cdot AlCl_3$/DEAC catalyst as follows: In the absence of H_2, the polymer chain cannot migrate from the active center because it contains a double bond at its end that is capable of forming a π-complex with the titanium center, thereby preventing the next growth step. When termination by hydrogen occurs, the polymer chain end is saturated and complexation cannot occur.

Particle Size Distribution

Cumulative particle size distributions (PSD) for the original catalyst and for polypropylene particles at different reaction times are shown in Figure

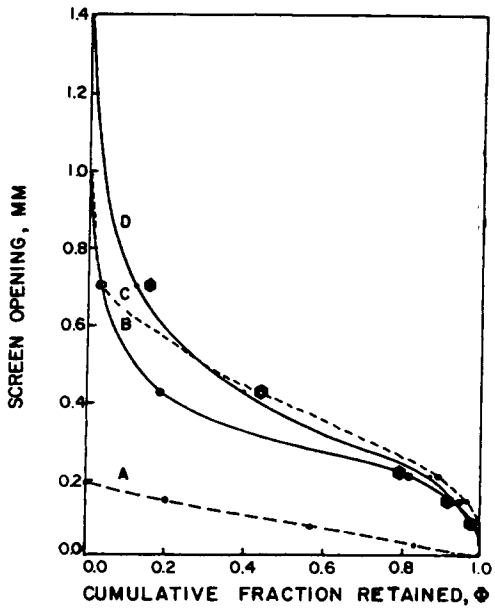

Fig. 14. Effect of reaction time on polymer particle size distribution (slurry polymerization data were taken from Ref. 24,) 70°C, 7.5 atm, [Al]/[Ti] = 3.68: (A) original catalyst; (B) t_f = 0.5 h; (C) t_f = 2.0 h; (D) t_f = 4.0 h; (●) slurry polymerization, 70°C, 13.9 atm., 4.0 h.

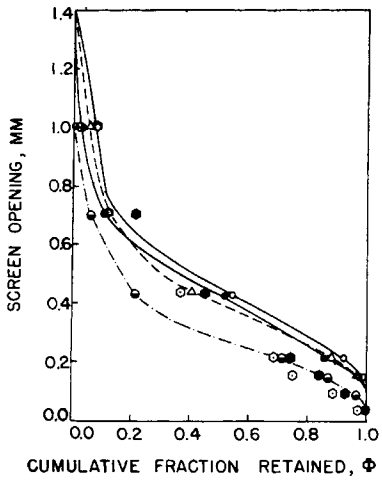

Fig. 15. Effect of temperature on polymer particle size distribution (slurry polymerization data were taken from Ref. 24), 7.5 atm. [Al]/[Ti] = 3.68. Temperatures (°C): gas phase: (◒) 32; (●) 50; (△) 70; (○) 90; slurry: (◉) 50; (●) 60.

14. Note that polymer particles grow most rapidly during the early stages of polymerization and the PSD changes very slowly after 2 h of reaction. It is also interesting to observe that the PSD for gas phase polymerization is quite similar to the PSD for liquid slurry polymerization using the same catalyst.[24]

The effect of reaction temperature on the PSD is shown in Figure 15. Although the polymer particle size is small at very low reaction temperatures (e.g., 32°C), the PSD is only slightly affected by temperatures above 50°C. PSD data for high pressure heptane slurry polymerization over the same catalyst system (taken from Ref. 24) indicates that there is a larger fraction of very small particles for slurry polymerization than for gas phase polymerization.

Figure 16 illustrates the theoretical and observed particle replication factors ($\gamma \equiv r_p/r_c$) and observed yield values. The average particle size of

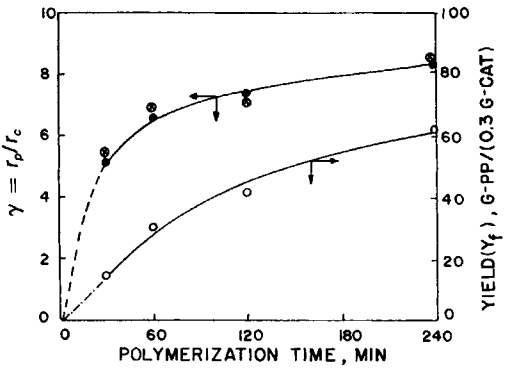

Fig. 16. Particle replication factor and yield as a function of reaction time; (⊕, ○) experimental values; (●) theoretical values calculated from rate data; P = 7.5 atm, 70°C, [Al]/[Ti] = 3.68.

the polymer was experimentally determined by sieve analysis and the theoretical average particle size (denoted by ●) was estimated from the observed polymer yield values. The particle size distribution of the original catalyst used is relatively narrow and the r_c value was taken from Ref. 29. The γ value after 4 h of reaction is well into the regime of industrial polypropylene manufactured using similar AA type catalysts (i.e., γ = 7–10).

Decay of Polymerization Rate

Decay in rate of polymerization is one of the prominent characteristics of propylene polymerization over heterogeneous Z—N catalysts (cf. Figs. 2, 5, and 8). Although many investigators have performed experiments to learn more about this phenomenon, there is still a lack of understanding of the fundamental mechanism. In the literature the observed decline in polymerization rate has been attributed to a number of factors: (1) deactivation of active sites; (2) nonisothermal effects during the early stages of reaction; or (3) intraparticle monomer diffusion resistances. We shall evaluate these possible mechanisms in what follows.

Let us assume first order rate of polymerization

$$R_p = k_p(T)[C^*][M]_s \tag{8}$$

where $[M]_s$ denotes the monomer concentration at the active catalytic sites. If the polymerization is carried out at constant temperature and pressure (i.e., semibatch experiment) without a loss of catalytic activity, the reaction rate should remain unchanged with time. However, R_p is observed to decrease with time with Z—N catalysts.

Caunt[30] postulated that excess $Al(C_2H_5)_2Cl$ cocatalyst acts as a poison while Keii and co-workers[23,31,32] have attributed the rate decay to a second-order deactivation of active polymerization centers resulting in the reduction of Ti(3+) to Ti(2+).

Choi et al.[15,33,34] have shown that poor heat dissipation from the small catalyst particle can cause a rapid rate increase with significant particle overheating during the very early stages of polymerization. However, this thermal effect lasts about 1–5 minutes, which is considerably shorter than the experimentally observed decay period (~1 h).

It has also been shown that increased diffusion resistance to monomer penetration into the growing polymer particle can cause a decrease in rate by reducing the effective monomer concentration at the active sites.[2,35–41] In particular, Taylor et al.[2] show that a reported rate constant (k_p) value derived from even short time polymerization data could be too low by a factor of 8–10 due to severe diffusion limitation during the early period of reaction. However, this effect takes place in a few seconds[2] and does not produce the slowly decaying reaction rates observed experimentally.

To observe the rate decay phenomenon, we carried out an interruption experiment similar to that performed by Doi et al.[23] As shown in Figure 17, propylene was replaced by nitrogen during the polymerization, and, after about an hour of intermission, propylene was reintroduced to resume polymerization. Note that the rate decay seems to continue during the

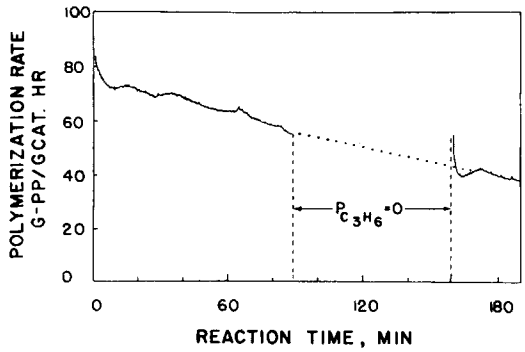

Fig. 17. Interrupted polymerization experiment showing catalyst deactivation of polymerization, 70°C, [Al]/[Ti] = 5.0, $P_{C_3H_6}$ = 7.5 atm.

intermission, suggesting that deactivation occurs even in the absence of polymerization.

If the reaction temperature and pressure are held constant, eq. (8) indicates that rate decay should be due to a decrease in [C*]. When a first-order deactivation mechanism is assumed, i.e.,

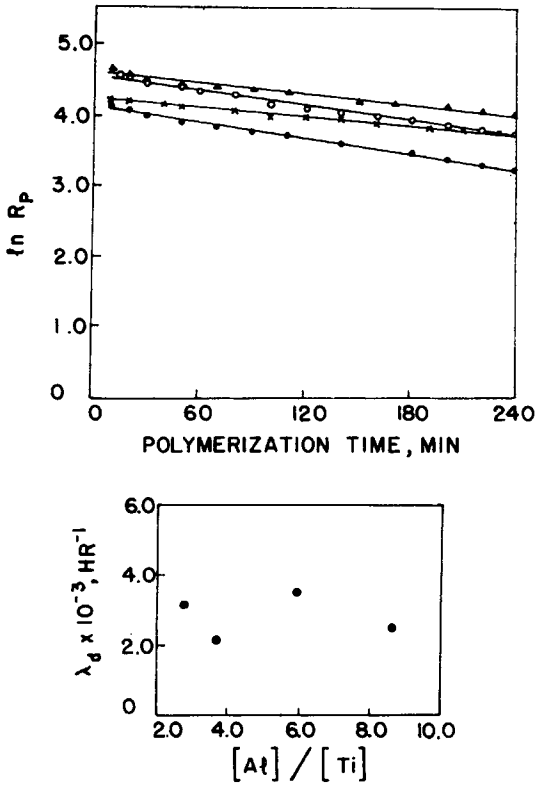

Fig. 18. Effect of [Al]/[Ti] (Stauffer AA 1.1/DEAC) ratios on catalyst deactivation, P = 7.5 atm, T = 70°C: (●) 2.76; (x) 3.68; (○) 5.90; (▲) 8.60.

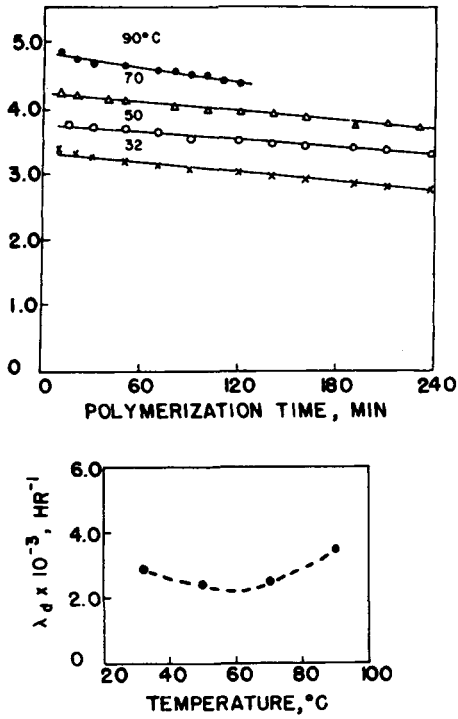

Fig. 19. Effect of temperature on catalyst deactivation, $P = 7.5$ atm, [Al]/[Ti] = 3.68.

$$\frac{d[C^*]}{dt} = -\lambda_d(\text{Al,Ti,T,}\cdots)[C^*] \qquad [C^*(0)] = [C^*]_0 \tag{9}$$

eq. (8) can be rewritten as follows:

$$R_p = k_p(T)[M]_s[C^*]_0 \exp(-\lambda_d t) \tag{10}$$

or

$$\ln R_p = \ln(k_p[M]_s[C^*]_0) - \lambda_d t \tag{11}$$

where $\lambda_d(\text{Al,Ti,T,}\cdots)$ is a decay constant and $[C^*]_0$ is an initial site concentration which may be a function of catalyst composition and other variables [cf. eq. (3)]. Figure 18 shows ln R_p vs. t for various [Al]/[Ti] ratios. Note that the first-order decay law fits the reaction rate data very well and that the decay constant is not very sensitive to the [Al]/[Ti] ratio.

The effect of temperature on the rate of deactivation is shown in Figure 19. Although λ_d is relatively insensitive to temperatures in the range of 30–70°C, λ_d increases sharply at higher temperatures. The half-life of the catalyst estimated from Figures 18 and 19 is ~3–5 h, which is somewhat shorter than that reported for a BASF industrial catalyst (i.e., $t_{1/2} = 7.7$ h for $TiCl_3$–TEA).[14] Very recently, disguised deactivation data with unspeci-

fied $TiCl_3$/DEAC catalyst systems have been reported[42] and show first-order decay with a 2-h half-life.

CONCLUDING REMARKS

Experiments of gas phase propylene polymerization have been performed using Stauffer AA Type 1.1 catalyst with $Al(C_2H_5)_2Cl$ as a cocatalyst. It has been found that the overall activation energy for the gas phase reaction (E_a = 4–10 kcal/mol) is considerably smaller than that for liquid slurry polymerization. An apparent break in the Arrhenius curve at around 50°C was also observed. Simulation results using the multigrain model[15] indicate that diffusion resistance in the microparticles may cause the retardation of the reaction rate observed at high temperatures.

Analysis of the reaction rate data and interruption experiments show that a chemical deactivation process seems to occur during the course of polymerization. A first-order deactivation model fits the experimental data satisfactorily.

A forthcoming paper in this series will present molecular weight distribution data and a quantitative comparison of model predictions and experimental observations.

We are indebted to the National Science Foundation and Mobil Foundation for support of this research. Many helpful discussions with Norman Brockmeier, Hal Grams, Habet Khelghatian, and others at the Amoco Chemical R&D Laboratory are gratefully acknowledged. David Alexander, our undergraduate research assistant, was of great help in running the experimental reactor.

References

1. N. F. Brockmeier, *MMI Symposium Series No. 4,* Harwood Academic, New York, 1983, Part B, p. 671.

2. T. W. Taylor, K. Y. Choi, H. Yuan, and W. H. Ray, *MMI Symposium Series No. 4,* Harwood Academic, New York, 1983, Part A, p. 191.

3. K. Y. Choi and W. H. Ray, *J. Macromol. Sci. Rev., Macromol. Chem. Phys.*, 1984, to appear.

4. T. Keii and Y. Doi, *Asahi Glass Kogyogijitsu Shoreikai Rep.*, **29**, 95 (1976).

5. T. Kohara, M. Shinoyama, Y. Doi, and T. Keii, *Makromol. Chem.*, **180**, 2139 (1979).

6. T. Keii, in *Coordination Polymerization,* J. C. W. Chien, Ed., Academic, New York, 1975, p. 263.

7. Y. Doi, Y. Yoshimoto, and T. Keii, *Nippon Kagaku Zasshi,* **3**, 495 (1972).

8. A. Takahashi and T. Keii, paper presented at Japanese Chem. Soc. Annual Meeting, Tokyo, 1966.

9. Y. Doi, Y. Hattori, and T. Keii, *Int. Chem. Eng.*, **14**(2), 369 (1974).

10. I. Okura, K. Soga, A. Kojima, and T. Keii, *J. Polym. Sci., Part A-1,* **8**, 2717 (1970).

11. K. Soga, T. Keii, and Y. Murayama, *J. Polym. Sci., Part B,* **4**, 199 (1966).

12. T. Keii, K. Soga, and N. Saiki, *J. Polym. Sci., Part C,* **16**, 1507 (1967).

13. V. A. Grigorev, V. I. Pilipovskii, Z. V. Arkhipova, E. V. Eroteev, and G. A. Fedina, *Int. Polym. Sci. Tech.*, **1**(5), 73 (1974).

14. V. K. Wisseroth, *Chem. Z.*, **101**(6), 271 (1977).

15. K. Y. Choi, PhD thesis, University of Wisconsin, 1984.

16. H. G. Yuan, T. W. Taylor, K. Y. Choi, and W. H. Ray, *J. Appl. Polym. Sci.*, **27**, 1691 (1982).

17. D. Y. Peng and D. B. Robinson, *Ind. Eng. Chem. Fundam.*, **15**(1), 59 (1976).

18. G. Natta, G. Mazzanti, P. Longi, and F. Bernadin, *Chim. Ind. (Milan),* **41**, 519 (1959).

19. Y. Doi, H. Kobayashi, and T. Keii, *Nippon Kagaku Zasshi,* N **6**, 1089 (1973).

20. V. K. Wisseroth, *Kolloid Z.Z. Polym.*, **241**, 943 (1970).

21. V. K. Wisseroth, private communication, 1978.
22. N. F. Brockmeier, *Am. Chem. Soc. Symp. Ser.*, **104**, 201 (1979).
23. Y. Doi, M. Murata, K. Yano, and T. Keii, *Ind. Eng. Chem. Prod. Res. Dev.*, **21**, 580 (1982).
24. G. E. Mann, PhD thesis, University of Wisconsin, 1986.
25. A. Schindler, *J. Polym. Sci.*, **C4**, 81 (1963).
26. C. D. Mason and R. J. Schaffhauser, *J. Polym. Sci., Part B*, **9**, 661 (1971).
27. E. M. J. Pijpers and B. C. Roest, *Eur. Polym. J.*, **8**, 1151 (1972).
28. G. Guastalla and U. Giannini, *Makromol. Chem. Rapid Commun.*, **4**, 519 (1983).
29. Technical Bulletin, Stauffer Chemical Co., 1972.
30. A. D. Caunt, *J. Polym. Sci., Part C*, **4**, 49 (1963).
31. K. Soga, T. Keii, and Y. Murayama. *J. Polym. Sci., Part B*, **4**, 199 (1966).
32. T. Keii, K. Soga, and N. Saiki, *J. Polym. Sci., Part C*, **16**, 1507 (1967).
33. K. Y. Choi, T. W. Taylor, and W. H. Ray, *Proc. IUPAC Macro. Symp.*, Amherst, 1982, p. 240.
34. K. Y. Choi, T. W. Taylor, S. F. Floyd, and W. H. Ray, *J. Appl. Polym. Sci.*, (1985), to appear.
35. E. J. Nagel, V. A. Kirillov, and W. H. Ray, *Ind. Eng. Chem. Prod. Res. Dev.*, **19**, 372 (1980).
36. J. W. Begley, *J. Polym. Sci., Part A-1*, **4**, 319 (1966).
37. W. R. Schmeal and J. R. Street, *AIChE J.*, **17**(5), 1188 (1971).
38. D. Singh and R. P. Merrill, *Macromolecules*, **4**(5), 599 (1971).
39. J. R. Crabtree, F. N. Crimsby, A. J. Nummelin, and J. M. Sketchley, *J. Appl. Polym. Sci.*, **17**, 959 (1973).
40. J. C. W. Chien, *J. Appl. Polym. Sci., Poly. Chem. Ed.*, **17**, 2555 (1979).
41. T. W. Taylor, PhD thesis, University of Wisconsin, 1983.
42. J. F. Ross, *J. Appl. Polym. Sci.*, **28**, 3593 (1983).

Received March 15, 1984
Accepted July 11, 1984